A&A 383, 275–282 (2002)
DOI: 10.1051/0004-6361:20011685

Astronomy & Astrophysics

Fine structure and dynamics in a light bridge inside a solar pore

J. Hirzberger[1], J. A. Bonet[2], M. Sobotka[3], M. Vázquez[2], and A. Hanslmeier[1]

[1] Institut für Geophysik, Astrophysik und Meteorologie, Universitätsplatz 5, 8010 Graz, Austria
[2] Instituto de Astrofísica de Canarias, 38200 La Laguna, Tenerife, Spain
[3] Astronomical Institute, Academy of Sciences of the Czech Republic, 25165 Ondřejov, Czech Republic

Received 24 August 2001 / Accepted 26 November 2001

Abstract. A photometric analysis of the sub-structure of a granular light bridge in a large solar pore is performed. The data consist of a 66 min time series of white light images ($\lambda = 5425\,\text{Å} \pm 50\,\text{Å}$) of an active region NOAA 7886 obtained at the Swedish Vacuum Solar Telescope on La Palma, Canary Islands. The light bridge can be resolved into an assembly of small grains embedded in a diffuse background with an intensity of about 85% of the mean photospheric intensity ($I_{\rm phot}$). Following the temporal evolution of these sub-structures in their irregular motions inside the light bridge, proper motions with velocities up to $1.5\,\text{km}\,\text{s}^{-1}$ can be detected. Their lifetime distribution shows a maximum at 5 min and a second peak at approximately 20 min. The origin and the decay of these sub-structures is very similar to those of granules, i.e. fragmentation, merging and spontaneous origination from, and dissolution into, the background can be observed. Some of them are able to escape from the light bridge into the umbra where they cannot be distinguished from adjacent umbral dots. Generally, this study presents evidence that the observed phenomenon represents convective motions.

Key words. Sun: granulation – Sun: photosphere – sunspots – convection

1. Introduction

Time series of photometric solar surface data with high spatial resolution exhibit a wide variety of phenomena as a consequence of the non-linear dynamics of flow fields and magnetic fields in the lower photosphere. After describing the structure and the time evolution of the granulation pattern in quiet regions in Hirzberger et al. (1997, 1999a,b) and the dynamics of fine structures in an active region in Sobotka et al. (1999a), the present work is dedicated to the analysis of the internal structure and kinematics of a granular light bridge observed inside a large pore (a sunspot lacking the penumbra).

Sunspots are the locations of the strongest magnetic fields in the solar photosphere. However, the convective transport is not fully inhibited and bright structures are clearly visible (see Sobotka 1997, 1999; Vázquez 2001 for a summary of their properties).

The presence of umbral bright features (umbral dots and light bridges) can be explained theoretically either in terms of the cluster model, where the umbra is formed by a tight bundle of isolated thin flux tubes, separated by field-free columns of hot plasma (Parker 1979a,b; Choudhuri 1986), or in terms of magnetoconvection taking place in a coherent but inhomogeneous large flux tube. Numerical simulations of magnetoconvection (Weiss et al. 1996; Blanchflower et al. 1998) show that when increasing the intrinsic magnetic field strength up to the conditions present in a sunspot umbra, the flow structure becomes completely controlled by the magnetic field. Thus the convective cells are prevented from expanding. This leads to a pattern of small and roundish convective cells regularly ordered in a grid- or chain-like structure (umbral dots). For lower field strengths the magnetic field is dominated by the convective flows, so that the flow field becomes chaotic and the growing convective cells push out the magnetic field into narrow lanes that surround them. This might occur in the case of light bridges.

According to Vázquez (1973), the formation of so-called "photospheric light bridges" in sunspots or pores is a result of the decay of the spot and the restoration of the granular surface. A positive correlation between the brightness and upflow velocities was reported by Rimmele (1997), who considered it as evidence for the magnetoconvective origin of photospheric light bridges. A systematic reduction of the magnetic field strength in light bridges, compared with the surrounding umbra, was found by Beckers & Schröter (1969), Abdusamatov (1970), Kneer (1973), and more recently by Wiehr & Degenhardt (1993), Rüedi et al. (1995), and Leka (1997). The oscillations

Send offprint requests to: J. Hirzberger,
e-mail: jkh@igam06ws.KFUnigraz.ac.at

observed in light bridges are not in phase with those in the adjacent umbral cores (Aballe Villero et al. 1993); this supports the idea that, although the umbra and the light bridges are at the same level in the atmosphere, they are physically different structures.

The internal structure of light bridges can be granular or filamentary. According to their width, light bridges are classified as (Sobotka et al. 1994; Sobotka 1997):

- *Faint light bridges* (FLBs): these are narrow bright streamers, which do not split the umbra. Their brightness is similar to, or lower than, that of the penumbra. Granular FLBs show granule-like structures ($\approx 0\farcs5$ wide) similar by size to umbral dots and small granules observed in fields of abnormal granulation. Filamentary FLBs consist of moving elongated bright grains, which are similar to penumbral grains (Muller 1979).

- *Strong light bridges* (SLBs): broad structures ($>2''$) which cross the umbra, dividing it into two or more umbral cores. Their brightness is related to their width, and reaches photospheric values for the broadest ones. Granular SLBs (also known as "photospheric bridges"), show two different populations of granules. One family consists of structures of sizes similar to those of FLBs, and the other with granules similar in size to photospheric granules. The second family begins to dominate with increasing width. Filamentary SLBs have a structure similar to that of the penumbra.

In 1995 we were fortunate to get high-resolution time series of a large pore with an important amount of bright structures, what surely produced its rapid decay in a few days. In Sobotka et al. (1999a) we have studied the umbral dots of this pore and the adjacent granulation. Here we will report about a photometric and dynamic study of a faint granular light bridge crossing the pore.

2. Observations and data reduction

A time series of white-light images of a pore region (NOAA 7886, Solar Geophysical Data No. 612) close to the center of the solar disk (at $\mu = 0.92$) was obtained at the Swedish Vacuum Solar Telescope on La Palma, Canary Islands (see Scharmer et al. 1985). The observations were performed on 30 June 1995 using a broad-band filter in white light ($\lambda = 5425\,\text{Å} \pm 50\,\text{Å}$). The total length of the time series is 66 min and the image size is $57'' \times 48''$. Typically, we used an exposure time of 11 ms and the image scale was $0\farcs062$ pix^{-1}.

The system was configured to work as a real time frame-selection device with selection intervals of 15 s. Considering the time to store the data on the disc, the effective time spacing between two images was 20 s on average. A typical value for the rms contrast in a subfield of quiet granulation included in the images – after correcting for dark field and flat field – was 7.6%. Many images show fine structure close to the diffraction limit of the telescope at the working wavelength ($0\farcs24$).

After correcting for dark fields and flat-fields the images were carefully compensated for rotation of the field of view in the focal plane produced by the altazimuthal configuration of the telescope and for global shifts mainly resulting from the insufficient bandwidth in the active mirror servo response. Subsequently, the images were normalized to the mean value of the photospheric intensity (I_{phot}) and were corrected for the telescope profile (assumed diffraction limited) using a Wiener filter, $F(\nu)$ (see Collados & Vázquez 1987) of the following form:

$$F(\nu) = \begin{cases} \frac{1}{MTF(\nu)} & \text{for } \nu \le \nu_0 \\ \frac{MTF(\nu)}{MTF^2(\nu) + C \cdot (\nu - \nu_0)} & \text{for } \nu > \nu_0 \end{cases} \quad (1)$$

where ν denotes the spatial frequency and $MTF(\nu)$ is the theoretical modulation transfer function of the telescope aperture. $C \cdot (\nu - \nu_0)$ models the inverse of the signal-to-noise ratio (SNR). Thus, pure restoration is performed up to ν_0, i.e. the SNR is assumed to be infinity. Beyond ν_0 the restoration operates in combination with filtering of noise thus resulting in a smoothly decreasing function from the maximum of restoration achieved about ν_0 up to zero at the cut-off frequency. The steepness of this decrease is ruled by the value of C. The parameters ν_0 and C were determined by trial and error to achieve a maximum restoration together with the minimization of noise. The values $\nu_0 = 2.22$ arcsec^{-1} and $C = 0.9$ were the best compromise in our case. Our restoration does not compensate the effect of degradation induced by terrestrial atmospheric turbulence since we have no information about it. Accordingly, although we can expect little contribution from the atmosphere because of the excellent quality of our material, our results, as far as the photometric measurements are concerned, have to be considered as slightly underestimated.

After the restoration for the telescope profile a time series of sub-boxes (288 pix $\times$288 pix) containing the large pore of NOAA 7886 has been extracted. In order to minimize image distortions resulting from differential seeing, this time series has been destretched using local correlation tracking techniques (see November & Simon 1988) implemented by Molowny-Horas & Yi (1994).

The final step in the data reduction was to apply a subsonic filter to remove acoustic modes and virtual fast motions induced by seeing. We used a filter with the cut-off phase velocity set to 5 km s^{-1} (see Hirzberger et al. 1997 for a discussion).

The influence of the stray light in our measurements can be neglected. Sobotka et al. (1993) and Bonet et al. (1995), working with analogous observing parameters, i.e. the same telescope, similar wavelength, good transparency and excellent seeing, estimated the level of scattered light as less than 1% of the mean intensity of the undisturbed photosphere. A more detailed description of the observing campaign and the data reduction can be found in Sobotka et al. (1999a) and Fig. 1 shows one example of the completely reduced images from the time series containing the pore.

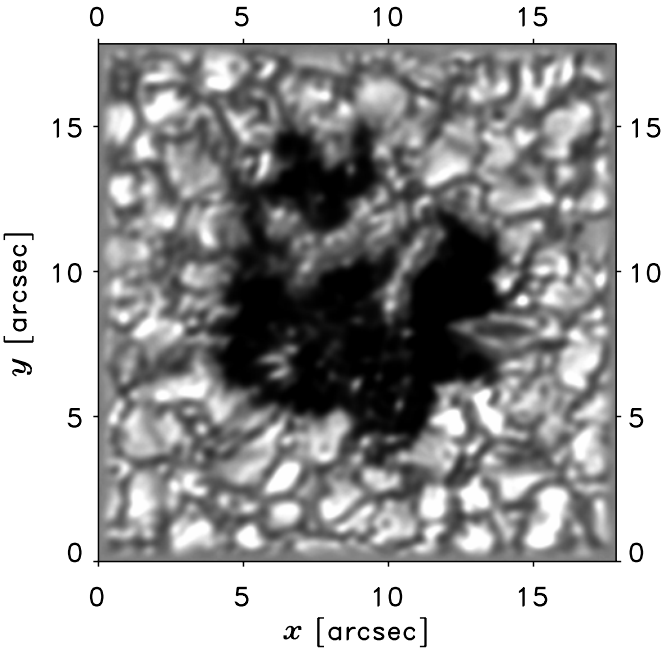

Fig. 1. White light image ($\lambda = 5425 \pm 50$ Å) of the large pore in NOAA 7886 after applying all pre-reduction procedures.

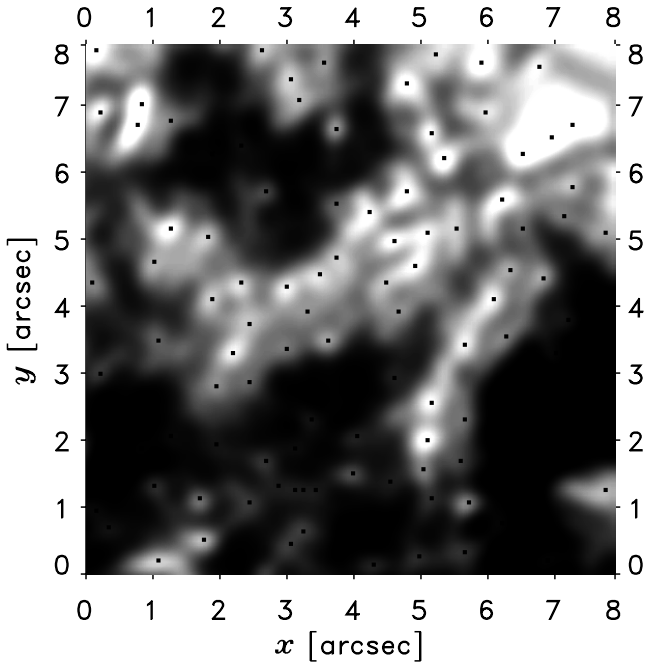

Fig. 2. Automatically detected (using a centre-finding algorithm) local intensity maxima in the region of the umbral light bridge.

3. Data analysis

The object of our study is a granular FLB with two arms, located in the pore (Fig. 1). It seems to be composed of an assembly of small and bright grains. Our first approach for an image segmentation separating these grains was to use an algorithm to detect their shapes automatically and track them in time as we have done for quiet granulation (see Hirzberger et al. 1997, 1999a). But since the size of these grains is close to the resolution limit of the data, the shapes detected by the algorithm were very sensitive to the quality of the images and therefore it was impossible to track them in time.

To avoid this problem, for detecting the grains in the light bridge automatically we used a centre-finding algorithm (see Title et al. 1989) after enhancing the contrast of the grains by unsharp masking; i.e., smoothing the images by a convolution with a Gaussian ($FWHM = 1\farcs32$) and subtracting the smoothed image from the original one. The centre-finding algorithm searches for pixels which are local intensity maxima, i.e. pixels where all surrounding pixels in each direction (vertical, horizontal and the two diagonals) are fainter than the one considered. An example of the result of this procedure is shown in Fig. 2. The intensity maxima in the light bridge visible by eye are well detected by this algorithm. This type of finding algorithm also detects local intensity maxima with very low absolute intensity values; i.e. it can also detect umbral dots. We have separated them from the grains in the light bridge assuming that they are fainter than $0.8\,I_{\rm phot}$.

The disadvantage of this method for detecting structures in the images is that it does not allow their sizes to be measured. We can obtain only their positions and their maximum intensities.

4. Results

The visual impression of the light bridge is that the bright grains seem to be embedded in a diffuse background which is brighter than the surrounding umbra. Since we observe features which are most probably below the resolution limit of the telescope, this background, observed with higher resolution would perhaps turn into narrow dark lanes surrounding the bright grains. To estimate this background intensity we have to define somehow the boundaries of single grains. Based on the inspection of the best resolved images we choose the value of 11 pix, i.e. $0\farcs68$ as a good compromise between the typical size of single grains and the average distance between them. We have then taken the maximum intensity, $I_{\rm max}$, of a grain as the intensity of the pixel detected by the finding algorithm and the observed minimum intensity of its surrounding background, $I_{\rm min}$, by the intensity of the darkest pixel in a circle of 11 pix diameter.

Histograms of $I_{\rm max}$ and $I_{\rm min}$ are plotted in Fig. 3. The curve for $I_{\rm max}$ shows a maximum almost exactly at $I_{\rm phot}$ and a sharp drop for higher intensities. Only very few of the grains (mainly those from the region close to the surrounding granulation) achieve intensities of $1.2\,I_{\rm phot}$. Additionally to the histogram of the maximum intensities of the grains in the light bridge a histogram of the maximum intensities of the umbral dots is plotted in Fig. 3. Both curves can represent a histogram of $I_{\rm max}$ of all the bright structures in the umbra. Since this second curve shows another significant maximum (approximately at $0.7\,I_{\rm phot}$) and since both curves fall to zero at $0.8\,I_{\rm phot}$, the two types of bright structures seem to be well

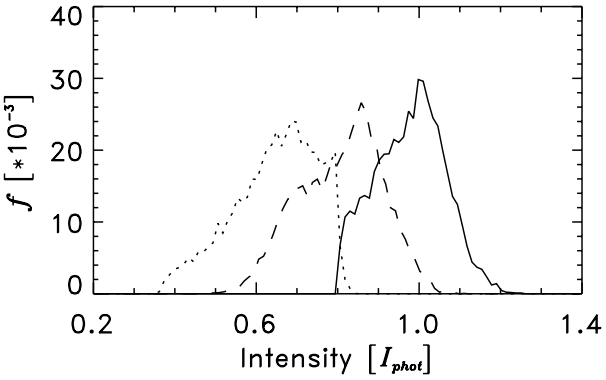

Fig. 3. Histograms of maximum intensities, $I_{\max}$ (*solid line*), minimum intensities, $I_{\min}$ (*dashed line*) of the grains in the light bridge and maximum intensities of umbral dots (*dotted line*). The minimum intensities were obtained from the darkest pixel in circles of diameter $0\farcs68$ around the detected intensity maxima. f denotes normalized number of elements.

separated by an intensity of $0.8\,I_{\rm phot}$ which was assumed as a threshold to discriminate them (see Sect. 3).

The histogram of $I_{\min}$ in the light bridge exhibits a maximum at $0.85\,I_{\rm phot}$ and a steep decrease towards higher intensities. The plateau between $0.65\,I_{\rm phot}$ and $0.75\,I_{\rm phot}$ is produced by those grains which are located at the borders of the light bridge. The rms intensity variations within the light bridge (inside a region with $I > 0.8\,I_{\rm phot}$ in the best image of the time series) amount to $6.55 \times 10^{-2}\,I_{\rm phot}$ which are 7.17% of the mean intensity ($0.913\,I_{\rm phot}$) in this region. The rms intensity variations of a quiet granular field of the the same image amount to 8.74%.

The tracking of the detected grains in the light bridge has been done manually. We have followed all the grains forward and backward in time starting at image number 60 (33 grains) and image number 135 (31 grains). The result from a statistics of the temporal evolution of these 64 grains is shown in Fig. 4. The distribution of the lifetimes, T, of the grains is shown in the left panel. The histogram exhibits a maximum at around $T = 5$ min and decreases for longer lifetimes with a significant secondary maximum at $T \approx 20$ min. In fact, the visual impression from looking at a movie of the light bridge is that the grains are quite long-lived, which is probably reflected in this secondary maximum. A typical lifetime of about 20 min for the grains of a granular SLB also has been found by Rimmele (1997). One of the tracked grains seems to be very long-lived. We were able to reach neither its birth nor its death. Therefore, we set its lifetime to $T = 66$ min, i.e. to the total length of the time series.

The mean velocity, v, of the grains was computed by first smoothing their trajectories (x_i, y_i) using a boxcar of 5 images' duration:

$$\overline{x}_i = \frac{\sum_{n=i-2}^{i+2} x_n}{5}\,, \qquad \overline{y}_i = \frac{\sum_{n=i-2}^{i+2} y_n}{5} \tag{2}$$

and, second, by averaging their x- and y-velocities

$$v_{x_i} = \frac{\overline{x}_i - \overline{x}_{i-1}}{t_i - t_{i-1}}\,, \qquad v_{y_i} = \frac{\overline{y}_i - \overline{y}_{i-1}}{t_i - t_{i-1}} \tag{3}$$

in time and computing the Pythagorean sum:

$$v = \sqrt{\langle v_x \rangle^2 + \langle v_y \rangle^2}\,, \tag{4}$$

where t_i is the time of the ith image. The smoothing of the trajectories had to be done for the reason that the distortion of the images by the seeing was not completely removed by the pre-reduction procedures although we have used the additionally destretched time series of sub-boxes (see Sect. 2). The histogram of the resulting mean velocities of the grains is plotted in the right panel of Fig. 4. It shows a peak at $250\,{\rm m\,s^{-1}}$ and a decrease towards higher velocities. From this histogram it can be seen that some of the grains seem to move with high velocities of more than $1\,{\rm km\,s^{-1}}$. These high velocities do not seem to originate from seeing effects. After smoothing the trajectories, all these effects should be removed. A confirmation of this result is given in Fig. 5, where the smoothed trajectories of the 64 tracked grains are plotted. Some of them move fast and almost straight ahead, whereas the motion of most of them seem to be quite irregular as in a random walk. In general, no preferred direction of the trajectories can be detected. The reason for this irregular motion might be that the grains are pushing against each other, which makes some of them moving fast straight ahead, whereas others are deflected when they run against another grain. The grains with the fastest motions are those which are able to escape from the light bridge.

An interaction of convective elements is also seen in quiet granulation. Numerical simulations of Stein & Nordlund (1998) indeed show that quiet granules are pushing against each other. Since the motions of the grains in the light bridge show a similar behaviour, this can be considered as an additional proof of their convective origin. On the other hand the large-scale motion of quiet granules is mainly determined by super- and mesogranular flow fields. In sunspot umbrae supergranular flows are inhibited by magnetic fields; hence, the motion of the convective elements inside the umbra can only be determined by the interaction with their nearest surroundings (i.e. adjacent grains and/or magnetic fields).

Another question that arises when tracking the grains in the light bridge is the nature of their "birth" and "death" mechanisms, i.e. at what stage of their evolution the tracking should be stopped. Our impression is that they behave very similarly to normal granules. We were able to find all the birth and death mechanisms that can also be seen for granules: fragmentation, merging, and dissolution to and spontaneous appearance from the background. The only problem that we have is that sometimes, when they are born or die, they are smaller in size or closer to each other than the resolution limit of our data. Hence, for many of them we cannot distinguish whether they dissolve into the background or become absorbed by a bright

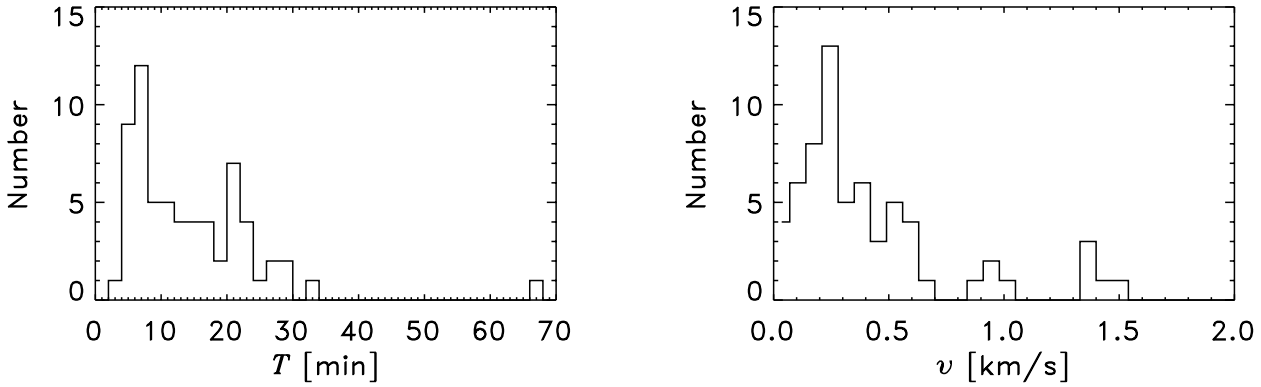

Fig. 4. Histograms of lifetimes, T (*left panel*), and mean velocities, v (*right panel*), of the 64 tracked grains in the light bridge.

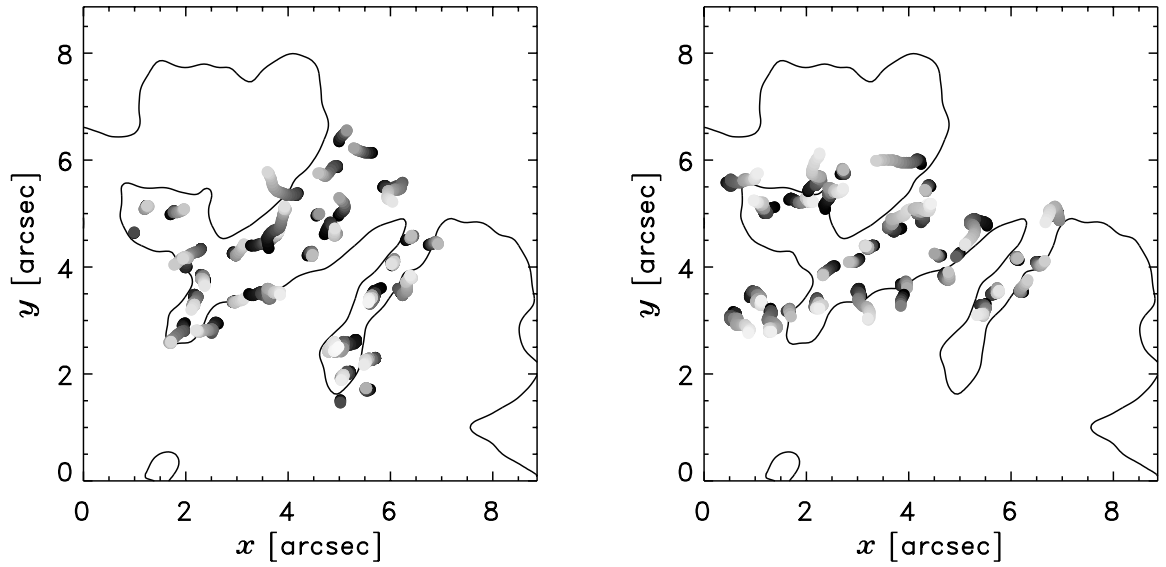

Fig. 5. Smoothed trajectories of the grains in the light bridge. In the *left panel* those grains where the tracking was started in image number 60 and in the *right panel* those grains where the tracking was started in image number 135 are displayed. The dark ends of the trajectories denote the positions of the birth of the grains; the bright ends correspond to the positions of their death. The contour lines correspond to 75% of the photospheric intensity in a summation of all the images of the time series.

adjacent grain (merge). In Fig. 6 three examples of dying grains are shown: the first (*upper panels*) is clearly splitting, the second (*central panels*) is dissolving into the background, and the third (*lower panels*) seems to merge with a large and bright neighbouring grain.

Dissolving grains can be classified into two different types. If the grain is pushed out of the light bridge into the umbra it can be followed until it reaches the intensity level of the umbra itself, which is – due to its rich internal structure – around $0.5\,I_{\rm phot}$ on average with minimum intensity values close to $0.34\,I_{\rm phot}$. Those grains which remain in the light bridge can be followed only until they reach the background intensity of the bridge, which is much higher than that of the umbra.

Another significant phenomenon can also be seen in Fig. 6 (*upper panels*). The grains in the light bridge sometimes tend to be ordered regularly in chains of more than two arcseconds in length; i.e. these chains sometimes contain five or more grains. This regularity is a transitory effect and the chain decays after a few minutes, but this spontaneous arrangement can recur many times in the light bridge but not always exactly at the same position.

An impression of the evolution in the light bridge can be also gained from the time-slices shown in Fig. 8. Two straight lines ("slits") were put on the two main arms of the light bridge (see Fig. 7) and the time evolution of the structures covered by the two lines is followed. The first time-slice (which lies across the major arm of the light bridge) shows that the grains can behave very differently. The very large and bright feature which is located between $x = 2\farcs8$ and $x = 4\farcs2$ (at $t = 0$) grows and decays in several steps almost like a quiet granule. (An alternative explanation for this behaviour might be that the feature is moving in and out of the "slit" but it has been checked that this definitively does not happen in this case.) The fainter small grain located at $x = 2\farcs3$ seems to

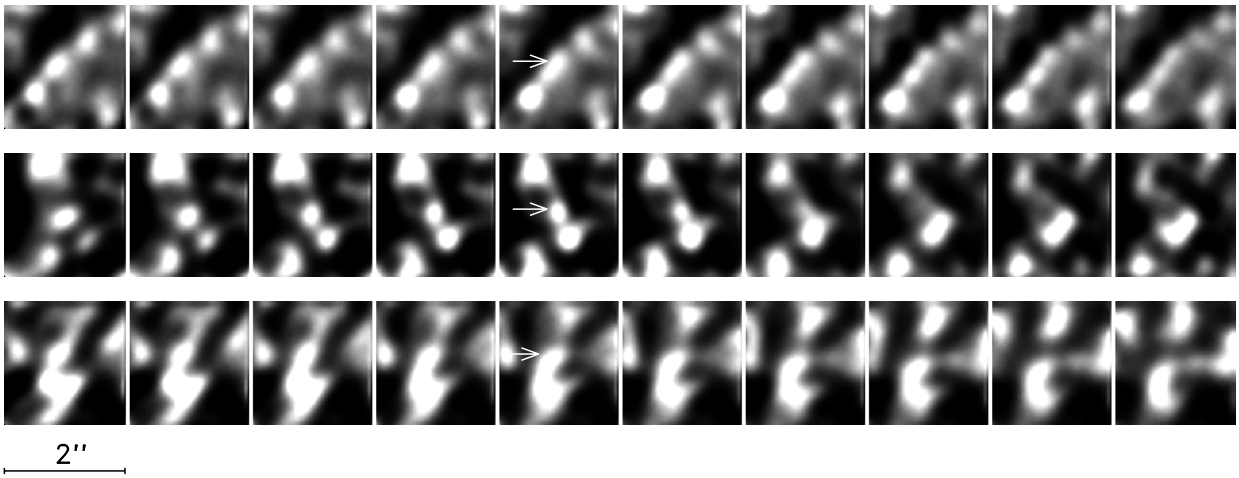

Fig. 6. Three examples of the death of grains in the light bridge. The *upper panels* show a clear fragmentation, the *central* story shows a dissolution into the background, and in the *lower panels* a merging of two grains can be seen.

be very long-lived but fragments into several other grains, which cover almost the total length of the light bridge after about 60 min. This event shows impressively how a spontaneous arrangement of the small grains can develop. At the inner end of the light bridge (at $x = 1\farcs3$) a very stable structure can be seen that has a lifetime of more than 30 min and does not seem to move at all within this time.

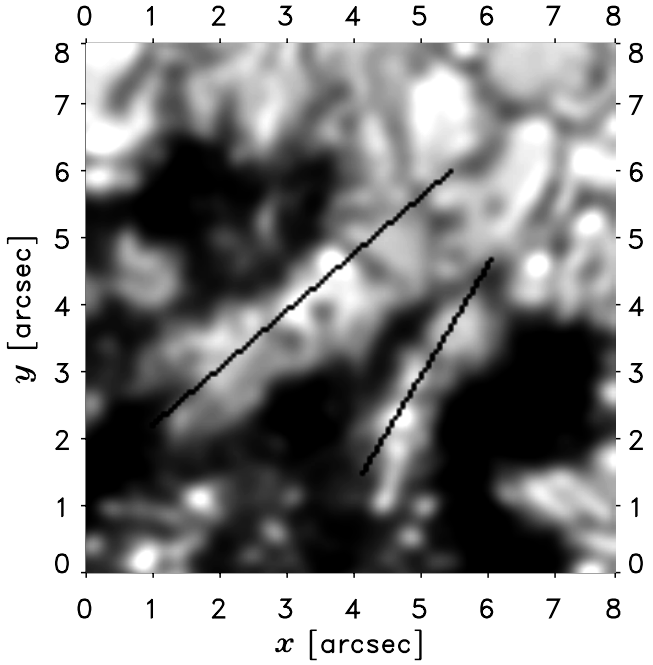

Fig. 7. Positions of the straight lines chosen for the two time-slices (shown in Fig. 8) in the first image of the time series.

The grains in the minor arm of the light bridge (the second time slice in Fig. 8) show much less dynamics than those in the other arm. The reason for this might be that this arm is much narrower and the evolution of the grains in inhibited by the high magnetic field strength in the surrounding umbra. The only event that we can see is a splitting of the bright grain at $x = 2\farcs7$ at $t = 4$ min.

Both time-slices in Fig. 8 show that the dynamics of the outer part (close to the edge of the pore) of the light bridge is more similar to that of quiet granulation than its inner part. This means that the size of the grains decreases and their lifetime increases the deeper they are located in the umbra. This is in good agreement with the model simulations of Weiss et al. (1996) and Blanchflower et al. (1998) if it is assumed that the magnetic field strength is higher in the inner end of the light bridge than in its outer end. Measurements of Rüedi et al. (1995) show that the field strength in SLBs is about 1500 G lower than in the surrounding umbra. Qualitatively similar results have also been found by Beckers & Schröter (1969), Abdussamatov (1970) and Kneer (1973).

5. Discussion and conclusions

We have observed time series of images of a pore region close to the centre of the solar disc. One of the pores in our images contains a relatively large FLB (see classification in Sect. 1) with two arms. Due to the excellent quality of our data the light bridge can be resolved into small grains. Formerly, light bridges have been studied in sunspots (e.g. Sobotka et al. 1993), and the present work is the first time that a detailed study is done in pores. However, we think that, basically, the properties of this FLB can be extrapolated to FLBs is mature sunspots.

Lifetimes, velocities and trajectories have been derived by tracking individual grains in the light bridge along the series of images. The histogram of lifetimes shows a maximum at $T = 5$ min and a significant secondary peak at 20 min. One of the tracked grains survives all through the whole time series.

The histogram of mean velocities exhibits a maximum at $250\,\mathrm{m\,s^{-1}}$ but grains moving faster than $1\,\mathrm{km\,s^{-1}}$ are also found. Most of the grains move in irregular

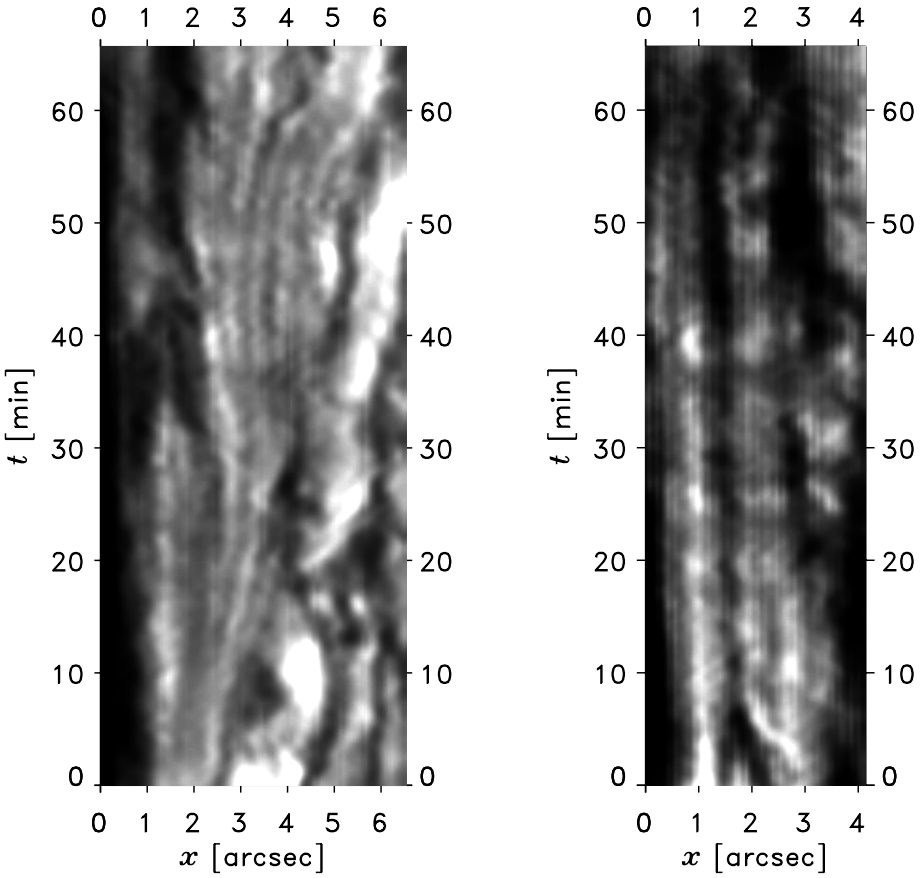

Fig. 8. Time-slices of the two main arms of the light bridge. $x = 0$ corresponds to the end of the light bridge closer to the centre of the umbra. The *left panel* shows the evolution of the major arm and in the *right panel* the evolution of the minor arm is displayed.

trajectories as in a random walk but some of them move fast and almost straight ahead.

From observations by Rimmele (1997), it may be concluded that the bright grains of light bridges correspond to convective cells because their intensity is well correlated with local vertical upflows, whereas in the darker lanes between the grains downward motions were found. Sobotka et al. (1994) have computed two-dimensional power spectra of light bridges. The slopes of these power spectra indicate the presence of a Kolmogorov turbulent cascade, although this diagnostic tool has been criticized as a numerical artefact by Nordlund et al. (1997).

Also, our observations provide evidence that photospheric light bridges consist of convective cells. The grains of light bridges are – similarly to quiet granules – able to fragment, merge, or dissolve into the background (see Fig. 6) and their proper motion is more or less random like the irregular motion of granules. (In quiet granulation an additional proper motion produced by meso- and supergranular flows can be detected.) The dynamics of the grains in the light bridge close to the edge of the umbra is more similar to that of granules, whereas in the inner part of the light bridge the dynamics of the grains seems to be totally dominated by the magnetic field, leading sometimes to a very regular arrangement of the grains (see Fig. 6, *upper panels* and Fig. 8). This result agrees very well with numerical simulations of Weiss et al. (1996) and Blanchflower et al. (1998), who have shown that the structure of the convective cells is strongly dependent on the magnetic field strength.

Some of the grains in the light bridge can – as they move – penetrate very far into the umbra. If they do so, they hardly can be distinguished from umbral dots. A close similarity between umbral dots and light bridges has already been suggested by Parker (1979b). Comparable processes have been observed by Sobotka et al. (1999a), using the same material as in this paper, with photospheric granules entering into the pore. Penumbral grains have also been observed entering into an umbra, and continuing there as umbral dots (Sobotka et al. 1995, 1997b).

The brightness structure of the light bridge makes it look as if the bright grains are sitting in a diffuse background that is much brighter than the surrounding dark umbra and does not change its shape very much throughout the entire time series.

Another remarkable feature of our light bridges is that the rms intensity fluctuations inside the light bridge are with 7.17%, considerably lower than in quiet granulation (8.74%). A reduction of the intensity contrast can also be detected when comparing abnormal with quiet

granulation. In former studies of abnormal granulation (e.g. Dunn & Zirker 1973; Bonet et al. 1984; Title et al. 1989; or Brandt & Solanki 1990) it is usually mentioned that the rms intensity fluctuations are smaller than in regions of quiet granulation. Thus it might be concluded that the presence of magnetic fields reduces the intensity fluctuations of a convective pattern. This might be explained by a reduction of the cell sizes and distances, which causes lateral radiative heating of the surroundings of small convective elements.

The histogram of grain speeds in light bridges looks very similar to that of inward penumbral grains (Sobotka et al. 1999b), but the corresponding lifetimes are much longer for the latter structures, and also for umbral dots (Sobotka et al. 1997a), although the shape of the distribution is similar.

In short, we have a common physical process, the modification of the granulation by surface magnetic fields. The resulting effect depends on the strength and geometry of the magnetic field. The transition between abnormal granulation, light bridges, penumbral grains and umbral dots has not clearly been established yet, both from the modeling and observational points of view.

Acknowledgements. The support provided by R. Kennerdahl and G. Hosinsky during the observations is gratefully acknowledged. This paper has been revised for English and style by the Scientific Editorial Service of the IAC. The SVST is operated on the island of La Palma by the Royal Swedish Academy of Sciences in the Spanish Observatorio del Roque de los Muchachos of the Instituto de Astrofísica de Canarias. This work was partially funded by the Spanish DGES project 95-0028, the Austro–Spanish "Acciones Integradas" HU93-013 and HU1997-0028, and by the Academy of Sciences of the Czech republic (Key Project K-2043105 and Grant A 3003903). JH, MS, and AH thank the IAC for their financial support and hospitality.

References

Aballe Villero, M. A., Marco, E., Vázquez, M., & Garcia de la Rosa, J. I. 1993, A&A, 267, 275
Abdusamatov, Kh. I. 1970, Sov. Astron. AJ, 14/1, 64
Beckers, J. M., & Schröter, E. H. 1969, Sol. Phys., 10, 384
Blanchflower, S. M., Rucklidge, A. M., & Weiss, N. O. 1998, MNRAS, 301, 593
Bonet, J. A., Márquez, T., Roca-Cortés, T., et al. 1984, in Proc. Sac. Peak Conf. on Small Scale Dynamical Processes in Quiet Stellar Atmospheres, ed. S. L. Keil, Sunspot NM, 323
Bonet, J. A., Sobotka, M., & Vázquez, M. 1995, A&A, 296, 241
Brandt, P. N., & Solanki, S. K. 1990, A&A, 231, 221
Choudhuri, A. R. 1986, ApJ, 302, 809
Collados, M., & Vázquez, M. 1987, A&A, 180, 223
Dunn, R. B., & Zirker, J. B. 1973, Sol. Phys., 33, 281
Hirzberger, J., Vázquez, M., Bonet, J. A., Hanslmeier, A., & Sobotka, M. 1997, ApJ, 480, 406
Hirzberger, J., Bonet, J. A., Vázquez, M., & Hanslmeier, A. 1999a, ApJ, 515, 441
Hirzberger, J., Bonet, J. A., Vázquez, M., & Hanslmeier, A. 1999b, ApJ, 527, 405
Kneer, F. 1973, Sol. Phys., 28, 361
Leka, K. D. 1997, ApJ, 484, 900
Molowny-Horas, R., & Yi, Z. 1994, ITA (Oslo) Internal Rep. No. 31
Muller, R. 1979, Sol. Phys., 61, 297
Nordlund, A., Spruit, H. C., Ludwig, H. G., & Trampedach, R. 1997, A&A, 328, 229
November, L. D., & Simon, G. W. 1988, ApJ, 333, 427
Parker, E. N. 1979a, ApJ, 230, 905
Parker, E. N. 1979b, ApJ, 234, 333
Rimmele, T. R. 1997, ApJ, 490, 458
Rüedi, I., Solanki, S. K., & Livingston, W. 1995, A&A, 302, 543
Scharmer, G. B., Brown, D. S., Petterson, L., & Rehn, J. 1985, Appl. Opt., 24, 2558
Sobotka, M. 1997, in Advances in Physics of Sunspots, ed. B. Schmieder, J. C. del Toro Iniesta, & M. Vázquez, ASP Conf. Ser., 118, 155
Sobotka, M. 1999, in Motions in the Solar Atmosphere, ed. A. Hanslmeier, & M. Messerotti (Dordrecht: Kluwer), 71
Sobotka, M., Bonet, J. A., & Vázquez, M. 1993, ApJ, 415, 832
Sobotka, M., Bonet, J. A., & Vázquez, M. 1994, ApJ, 426, 404
Sobotka, M., Bonet, J. A., Vázquez, M., & Hanslmeier, A. 1995, ApJ, 447, L133
Sobotka, M., Brandt, P. N., & Simon, G. W. 1997a, A&A, 328, 682
Sobotka, M., Brandt, P. N., & Simon, G. W. 1997b, A&A, 328, 689
Sobotka, M., Vázquez, M., Bonet, J. A., Hanslmeier, A., & Hirzberger, J. 1999a, ApJ, 511, 436
Sobotka, M., Brandt, P. N., & Simon, G. W. 1999b, A&A, 348, 621
Stein, R. F., & Nordlund, Å. 1998, ApJ, 499, 914
Title, A. M., Tarbell, T. D., Topka, K. P., et al. 1989, ApJ, 336, 475
Vázquez, M. 1973, Sol. Phys., 31, 377
Vázquez, M. 2001, in Encyclopedia of Astronomy and Astrophysics (Nature Publishing Group), in press
Weiss, N. O., Brownjohn, D. P., Matthews, P. C., & Proctor, M. R. E. 1996, MNRAS, 283, 1153
Wiehr, E., & Degenhardt, D. 1993, A&A, 278, 584